

Pressurized electro-Fenton for the reduction of the environmental impact of antibiotics

Ángela Moratalla¹, Danyelle M. Araújo², Gabriel O. M. A. Moura³, Engracia Lacasa⁴, Pablo
Cañizares¹, Manuel A. Rodrigo¹, Cristina Sáez^{1*}

¹ Department of Chemical Engineering, Faculty of Chemical Sciences and Technologies,
University of Castilla-La Mancha, Edificio Enrique Costa Novella, Campus Universitario
s/n, 13005 Ciudad Real, Spain

² Faculty of Exact and Natural Sciences, State University of Rio Grande do Norte, Campus
Central, Mossoro - RN 59625-620, Brazil

³ Federal University of Rio Grande do Norte, School of Science and Technology, Natal -
RN, 59078-970, Brazil

⁴ Department of Chemical Engineering, Higher Technical School of Industrial Engineering,
University of Castilla-La Mancha, Edificio Infante Don Juan Manuel, Campus Universitario s/n,
02071 Albacete, Spain

*author to whom all correspondence should be addressed (corresponding author):

cristina.saez@uclm.es. Tel.: +34-926-29-53-00 Ext. 6708

22 **ABSTRACT**

23 This work evaluates the performance of a pressurized heterogeneous electro-Fenton (EF)
24 process to transform the antibiotic into compounds that do not promote the appearance of
25 bacteria resistant to antibiotic in the environment. Experimental system consisted of a
26 pressurized non divided microfluidic electrochemical cell equipped with a jet aerator, flow-
27 through electrodes and a fluidized bed of goethite as heterogeneous iron catalyst. Results show
28 that meropenem (model antibiotic) can be degraded by EF and that the degradation rate
29 depends on the gauge pressure applied: the higher is the pressurization, the faster is the
30 abatement of meropenem. The antibiotic effect of the urine is related to meropenem remained
31 in the treated urine, and the contribution of reaction intermediates does not seem to be relevant.
32 The mineralization of the organic load is almost nil. The higher dissolved oxygen
33 concentration of pressurized-EF and thus, the higher hydrogen peroxide generation seems to
34 be the key point to explain the effect of pressure on EF process. Results confirm that
35 moderated pressurized EF process (up to 3 bar) can be satisfactorily used to decrease the
36 chemical risk of synthetic hospital urines, which opens the possibility of an optimized pre-
37 treatment which may help to save cost in the treatment of these hazardous wastes.

38

39

40

41 **Keywords**

42 Antibiotic, urine, antibiotic effect, electro-Fenton, pressure.

43

44

45

46

47 1. INTRODUCTION

48 The presence of antibiotics in aquatic environments, related to its high consumption and the
49 inefficiency of conventional biological processes to remove this type of compounds, is one of
50 the main subjects of environmental concerns nowadays [1, 2]. Because of this, many
51 researchers have focused their studies on the development of technologies for the abatement
52 of this type of pharmaceutical compounds from industrial and treated urban wastewater to
53 prevent their accumulation in the environment. Recently, the focus has been on the treatment
54 of sanitary effluents that are considered one of the main routes of entry of antibiotics into the
55 environment.

56 During last decade, Electrochemical Advanced Oxidation Processes (EAOPs) have
57 demonstrated their readiness to reach high efficiencies in the degradation of organic
58 compounds, including antibiotics and other pharmaceuticals in different aqueous matrixes [3-
59 5]. Among EAOPs, EF process is one of the most effective technologies for achieving fast
60 and complete degradation of target organic pollutants in water [6-8]. This process is based on
61 the continuous electro-generation of hydrogen peroxide by reducing oxygen at the cathode,
62 and the activation of this oxidant throughout its transformation into hydroxyl radicals by the
63 decomposition of H_2O_2 catalyzed by Fe^{2+} through Fenton's Reaction. Then, the performance
64 of the EF process depends on the electroactivity and selectivity of the cathode to produce
65 H_2O_2 . Carbonaceous materials doped with a mixture of carbon black and
66 polytetrafluoroethylene (CB/PTFE) have demonstrated good results in the rapid and efficient
67 production of hydrogen peroxide [4, 9-14]. In addition, the oxygen fed, and the Fe-based
68 catalysts are also considered two key parameters in the development of efficient processes and
69 further scientific effort is still needed to design EF reactors feasible to be scaled and that allow
70 the implementation of the technology at full-scale.

71 To solve the problem of oxygen feeding, different strategies have been evaluated. In many
72 cases, gas diffusion electrodes (GDE) were used [15]. GDE allows air or oxygen to pass
73 directly through the diffusion layer, but it generally presents a relatively small specific
74 electrode surface area, poor stability, and difficult scalability. Because of this, some authors
75 have studied other alternatives. Pérez et al. [16] reported the use of a jet aerator based on the
76 Venturi effect, which allowed generate air bubbles and supersaturate in oxygen the electrolyte
77 without the need for a compressor. The jet was also used by Yu et al. [17] in a novel jet-type
78 reactor (vertical flow reactor) to enhance the hydrogen peroxide production, getting that the
79 H₂O₂ production was much larger than the traditional gas diffusion cathode (1419 mg dm⁻³
80 against 684 mg dm⁻³, respectively) and where the removal of tetracycline hydrochloride with
81 this novel reactor was around 100% (88% of total organic carbon, TOC) within the 60 min of
82 reaction in EF process. Other authors proposed the use of pressurized-EF reactors in which
83 the system was pressurised with air or oxygen to increase the dissolved oxygen concentration,
84 demonstrating that hydrogen peroxide generation can be significantly improved [11, 18, 19].
85 The obtained results showed that the removal of organics such Acid Orange 7 and maleic acid
86 was accelerated using air-pressurized EF processes [18, 20]. In addition, Klidi et al. [21]
87 reported the treatment of paper mill wastewater by pressurized-EF, improving TOC removal
88 from 48 to 58% when pressure increased from 1 to 10 bar. Similar results were obtained by
89 Ltaïef et al. [19].

90 With this background, this work tries to go one step further, proposing for the first time the
91 study of the influence of pressurization at bench scale on the performance of a heterogeneous
92 EF process in its application for the degradation of antibiotics in synthetic hospital urine,
93 selected as model of sanitary effluent where drugs are highly concentrated. In this case, the
94 complete mineralization of the organic load is not required, but the decrease of the
95 hazardousness associated to the polluted urine. That is, the aim is to transform the antibiotic
96 into compounds without antibiotic effect that do not promote the appearance of bacteria

97 resistant to antibiotic in the environment, but not their complete mineralization (which will be
98 cheaper by many other technologies). To do this, meropenem is selected as antibiotic model,
99 which is a broad-spectrum antibiotic of the carbapenem class that is frequently used to treat
100 clinical diseases caused by Gram-negative bacteria such as *Escherichia coli* (*E. coli*) [22] and
101 that is excreted through urine. The experiments are performed in a pressurized microfluidic
102 electrochemical cell equipped with a jet aerator and flow-through electrodes [11], and results
103 are evaluated in terms of meropenem abatement and removal of antibiotic effect.

104

105 **2. MATERIALS AND METHODS**

106 *2.1 Chemicals*

107 Meropenem trihydrate (MRP) was supplied by the Pharmacy Department of the Albacete
108 University Hospital (Spain). Anhydrous sodium sulphate (Na_2SO_4) was purchased from
109 Panreac. Calcium phosphate, diammonium hydrogen phosphate, sodium carbonate,
110 magnesium sulfate, potassium chloride, uric acid, creatinine, and urea were used to make the
111 synthetic urine and supplied by Sigma-Aldrich. The pH of the samples was adjusted using
112 sulfuric acid (H_2SO_4) and sodium hydroxide (NaOH). HPLC grade Methanol, HPLC grade
113 acetonitrile and formic acid (98% from Sigma-Aldrich) were used in the mobile phase. P-
114 dimethylaminobenzaldehyde (from Sigma-Aldrich) and titanium (IV) oxysulfate (1.9-2.1%,
115 from Sigma-Aldrich) were used as indicators of urea and hydrogen peroxide, respectively.
116 Goethite (catalyst grade, 30-50 mesh from Sigma-Aldrich) was used as heterogeneous catalyst
117 for EF tests. All solutions were prepared using double de-ionized water (Millipore Milli-Q
118 system, resistivity: $18.2 \text{ M}\Omega \text{ cm}$ at $25 \text{ }^\circ\text{C}$).

119 *2.2 Experimental set-up*

120 As shown in Figure 1a, the experimental setup consists in a microfluidic flow-through cell
121 (MF-FT) with a pressurized-jet aeration (PJA). The tank, the cell and the pipelining are

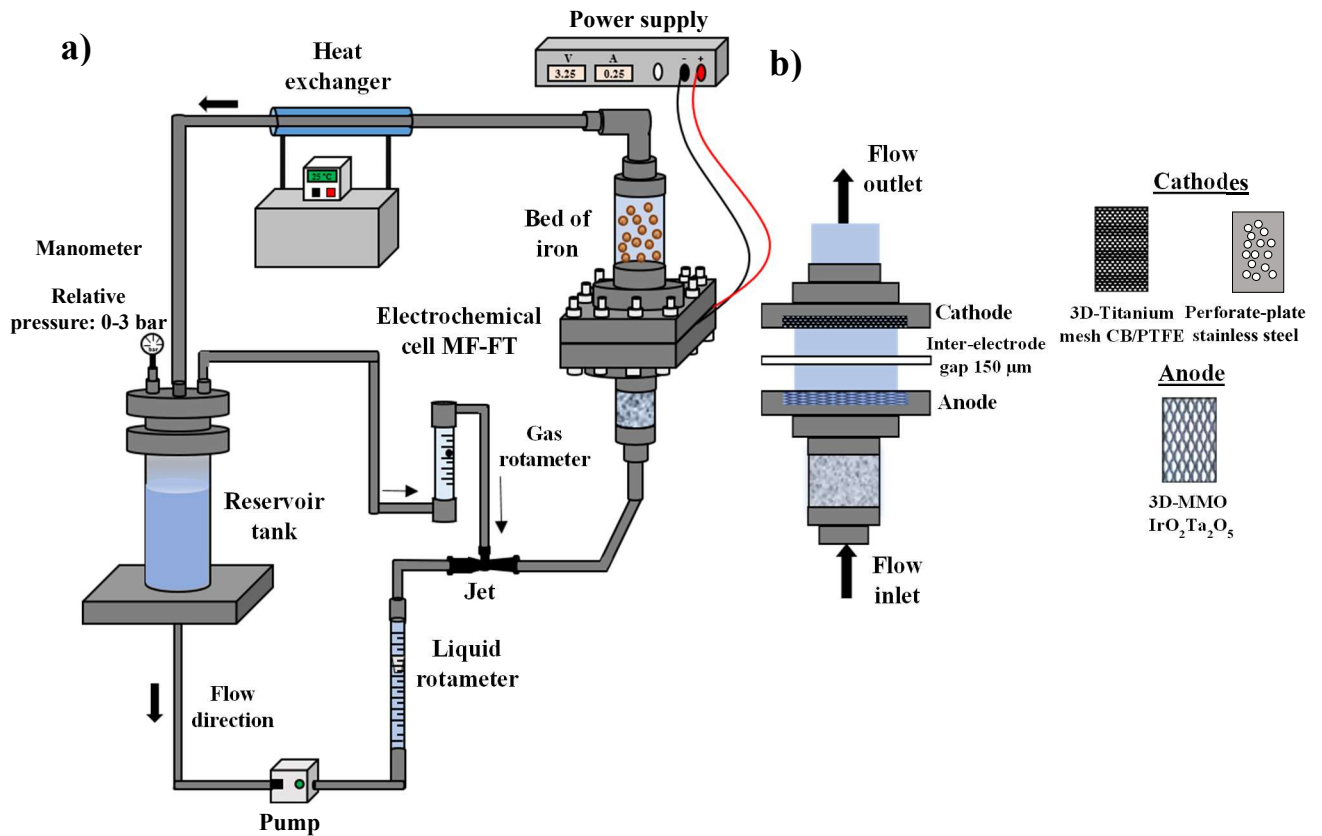
122 fabricated from polyvinyl chloride (PVC). The electrolyte (2.7 dm^{-3}) is fed to the cell from
123 the reservoir tank by a Micropump® (GB-P25 J F5 S A head coupled to a DB 380 A 24 V
124 motor with speed control 0-5 V DC supplied by Techma GPM s.l.r.) fixing a flow rate of 140
125 $\text{dm}^3 \text{ h}^{-1}$. In addition, it incorporates a fluidized bed of goethite particles connected to the outlet
126 of the electrochemical cell. The fluid velocity throughout the bed is 0.043 m s^{-1} . A heat
127 exchanger is used for control temperature.

128 In the MF-FT cell, the electrodes are separated by a polytetrafluoroethylene (PTFE) film with
129 an inter-electrode gap of $150 \text{ }\mu\text{m}$. 3D-Mixed Metal Oxide mesh (MMO- $\text{IrO}_2\text{Ta}_2\text{O}_5$) supplied
130 by Tianode® is used as anode. 3D-titanium mesh with a deposition of carbon black (CB,
131 Vulcan® XC72 from cabot corporation) and PTFE (a 60% wt. Teflon® emulsion solution in
132 H_2O , from Sigma-Aldrich) is used as cathode in EF tests. In Electrooxidation (EO) tests, the
133 cathode is replaced by a perforate-plate stainless steel AISI 304. (Figure 1b). The dimensions
134 of the electrodes were $8 \times 9.5 \text{ cm}$, with 33 cm^2 corresponding to the wet area. The surface area
135 was 49.5 cm^2 and was estimated by determining the surface/ geometric area ratio [23].

136 For cathode preparation, the titanium mesh (from Xian Howah Technology Co., Ltd.) is
137 immersed into boiling hydrochloric acid (HCl, 37% from Scharlab) solution (20% v/v) for 15
138 min, followed by immersion into boiling oxalic acid (99.5 % from Panreac) solution (10%
139 v/v), and finally it is rinsed with ultrapure water. The CB/PTFE mixture are prepared by
140 dispersing 1 mg mL^{-1} of CB and 5 mg mL^{-1} of PTFE into isopropanol for 2 hours at $50 \text{ }^\circ\text{C}$ in
141 an ultrasound bath. After this, titanium mesh is place over plate at $130 \text{ }^\circ\text{C}$ and 200 mL of ink
142 is sprayed (100 mL each side). Finally, electrodes are tempered at $360 \text{ }^\circ\text{C}$ for 1 h starting from
143 room temperature at a heating rate of $12 \text{ }^\circ\text{C min}^{-1}$. A second layer is deposited on the electrode,
144 repeating the procedure.

145 Synthetic urine is polluted with 50 mg dm^{-3} of meropenem. Urine consists of a mixture of
146 organic species such as urea, creatinine, uric acid, and inorganic salts (including potassium

147 chloride, magnesium sulfate, or diammonium hydrogen phosphate). The composition
 148 synthetic urine has been reported elsewhere [24]. The initial pH of the solution is adjusted to
 149 3.0. All experiments are carried out under galvanostatic conditions at a current density of 5.0
 150 mA cm⁻². The amount of goethite used in the fluidized bed is 10.8 g (it guarantees good
 151 fluidization of the goethite particles). In the different tests, the system is pressurized, and tests
 152 are carried out at gauge pressures ranging from 0.0 to 3.0 bar. The key of the pressurized
 153 system is connecting the intake of the jet aerator to the biphasic reservoir tank. After
 154 pressurization, the system is in equilibrium as in the case of jet aerated under room pressure.
 155 When liquid flows through the Venturi, a difference of pressure appears between the tank and
 156 the throat of the jet serving as the driving force (ΔP) to aspire the gas, but in this case a
 157 pressurized liquid-gas mixture is obtained. During the treatment the pressure variance is nil.
 158 In any case, any possible overpressure caused by gases generated during the process is
 159 removed when the system is momentarily opened for sampling.



160

161 **Figure 1.** Experimental set-up. a) Complete view, b) diagram of the electrochemical cell MF-FT and
162 electrodes.

163 *2.3 Analytical*

164 Meropenem, intermediates and uric acid concentrations are monitored via High Performance
165 Liquid Chromatography (HPLC) using Agilent 1100 series coupled a DAD detector and a
166 Zorbax Eclipse Plus C18 analytical column (4.6 mm x 100 mm; 3.5 μm). The mobile phases
167 used for the determination of meropenem are 15% acetonitrile and 85% formic acid (0.1%) at
168 a flow rate of 0.6 mL min^{-1} at 300 nm. The injection volume is 20 μL . On the other hand, uric
169 acid is determined by using a mobile phase consisting of 2% acetonitrile and 98% aqueous
170 solution with 0.1% of formic acid, applying a flow rate of 1.0 mL min^{-1} , an injection volume
171 of 20 μL and 292 nm wavelength.

172 Intermediates are identified on an Agilent 1260 Infinity coupled to an Agilent time-of-flight
173 mass spectrometer (LC-MS TOF 6230) with an electrospray interface operating under the
174 following conditions: capillary, 3500 V; nebulizer 40 psi; drying gas, 10.0 L/min; gas
175 temperature, 325 $^{\circ}\text{C}$; skimmer voltage, 65 V. Mobile phase is composed of 15% acetonitrile
176 and 85% aqueous solution with 0.1% formic acid, and flowed at 0.6 mL min^{-1} through a
177 Zorbax Eclipse Plus C-18 column (4.6 mm x 100 mm; 3.5 μm).

178 The urea is estimated by a spectrophotometric colorimetric method using a UV-1700
179 Shimadzu Spectrophotometer according to the previously reported methodologies [25].

180 Creatinine, anions and cations are determined via ion chromatography (IC) with a Metrohm
181 930 Compact IC Flex coupled to a conductivity detector. Organic acids are identified by
182 HPLC using a Jasco 2080 Plus equipped with a Hi-Plex H (7.7 mm x 300 mm; 8 μm) with
183 detection at 210 nm. The mobile phase consists of 5 mM H_2SO_4 and the injection volume is
184 20.0 μL . The hydrogen peroxide concentration is measured by spectrophotometric method,
185 following the concentration of the complex formed between H_2O_2 and Ti^{4+} [26].

186 The iron concentration in EF tests is measured using an inductively coupled plasma atomic
187 emission spectroscopy in a Varian Liberty RL sequential ICP-AES equipment.

188

189 *2.4 Antibiotic activity assay*

190 The antibiotic activity of initial and final meropenem samples is determined by using
191 Microtrac[®] 4200 that counts the colony forming units (CFU) per mL. The microorganism used
192 as indicator is *E. coli*. Before antibiotic activity assay, the microorganisms are incubated on
193 plates with a selective agar at 37 °C for 24 h. Consequently, urine solution without antibiotic
194 is contaminated with 10⁷ CFU of *E. coli*. To verify the initial population of *E. coli*, a control
195 sample (blank) is measured. After this, the antibiotic activity assays are conducted in beakers
196 where 5 mL of urine samples taken from the solution under treatment are added to 5 mL of
197 the solution containing the microorganism. It is maintained under continuous agitation for 3
198 h at 37 °C. Finally, 1 mL is taken to a measurement cell with culture medium and introduced
199 to the equipment to perform the CFU count. Each urine sample is measured by quadruplicate:
200 without dilution and with dilution 1:10, 1:100 and 1:1000.

201

202 **3. RESULTS AND DISCUSSION**

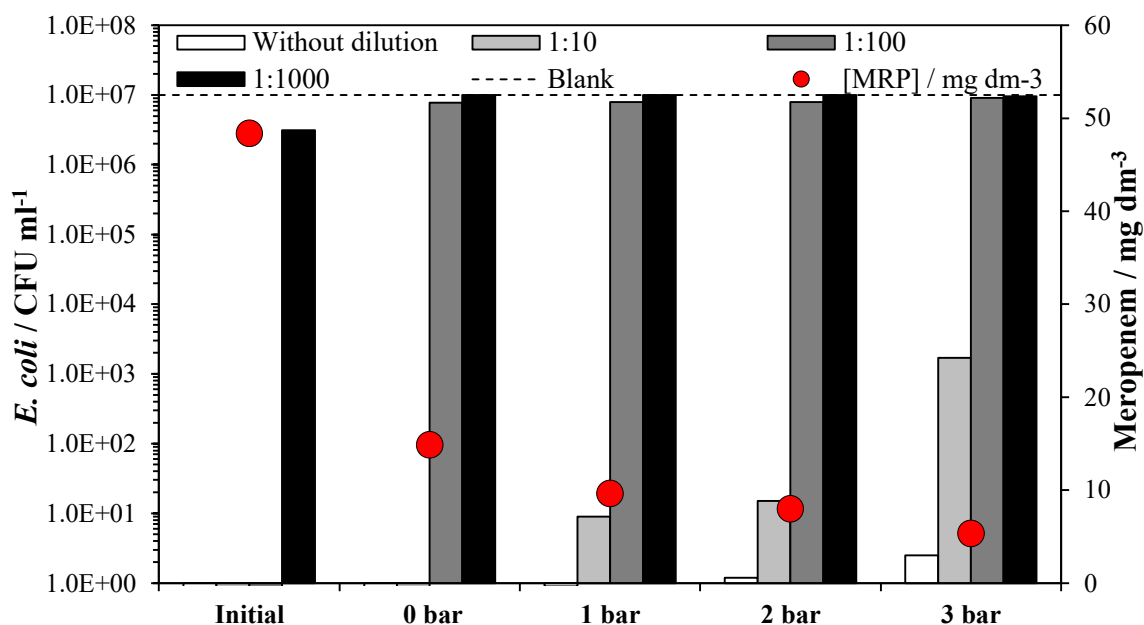
203

204 Figure 2 shows the final concentration of meropenem remained in the urine after 6.0 h (0.6
205 Ah L⁻¹ of electric charge passed) of treatment by EF at different pressurization (gauge
206 pressures ranging from 0 to 3 bar). Additionally, the antibiotic effects of the initial and treated
207 urines are also plotted in terms of CFU of *E. coli* per mL. This antibiotic effect is measured
208 indirectly by comparing the effect of addition of the treated and non-treated urine on a culture
209 of *E. coli*: the higher the number of colonies that survive in the urine, the lower the antibiotic
210 capacity of the urine. In all cases, an initial population of 10⁷ CFU mL⁻¹ of *E. coli* is used, and

211 each urine sample (taken from the solution under treatment) is measured by quadruplicate
212 (without dilution and up to 1:1000 dilution). Before starting, pH values were adjusted to 7.0
213 and the oxidants potentially formed during the electrochemical process (such as hydrogen
214 peroxide, hypochlorite...) were neutralized with thiosulfate. As well, a reference test in
215 absence of antibiotic is carried out to confirm that *E. coli* is not sensitive to other compounds
216 naturally present in the urine and, thus, to discard possible interferences. Thus, it is expected
217 that the obtained results only inform about the antibiotic effect of meropenem, and its reaction
218 intermediates generated during treatment. As well, to show the sensitivity of *E. coli* to
219 meropenem in the conditions used in this work, data obtained with the raw polluted urine
220 (without treatment) are also included in the Figure.

221 As it can be observed, the meropenem contained in the raw urine (50 mg dm^{-3}) can eliminate
222 completely the *E. coli* contained in the testing samples, and only few colonies can survive
223 when 1:1000 dilution of the raw urine is tested. This confirms that *E. coli* can be used as target
224 model bacterium to monitor the antibiotic activity of synthetic urines polluted with
225 meropenem. Regarding urine samples taken after EF treatment, results show that
226 heterogeneous EF can decrease the meropenem concentration as well as the antibiotic effect
227 of the urine. It is important to take in mind that degradation of the raw antibiotic can lead to
228 the formation of species which still have antibiotic capacity, whose discharge into the
229 environment may favour the development of antibiotic resistant cultures in the environment.
230 Additionally, it can be noted that the increase in the gauge pressure influences markedly on
231 the two parameters selected to monitor the treatment tracking: the higher is the gauge pressure
232 applied during the EF, the higher is the removal of meropenem and the higher is the survival
233 of *E. coli*. This direct relationship between the decrease in the concentration of the antibiotic
234 and the survival of *E. coli* is expected because of the antibiotic capacity of the raw molecule.
235 However, this later parameter is more valuable because it informs also about the antibiotic
236 capacity of the degradation products. In comparing the trends of both parameters, it can be

237 seen that the effect of the pressurization on the removal of meropenem is lower than in the
238 antibiotic effect, suggesting an influence of the formation of intermediates in this later
239 parameter and the necessity of the simultaneous measurement of the two parameters to
240 understand what it is really happening inside the reactor. In this point, it is important to point
241 out that the minimum inhibitory concentration (MIC) of meropenem to *E. coli* is below 2.00
242 mg dm⁻³ [27] and, therefore, in urine polluted with lower concentrations no effect should be
243 expected and *E. coli* should remain almost unaltered in the urine media. This is observed in
244 the EF carried out at 3 bar of gauge pressure, where the final meropenem concentration is
245 closer to the MIC and some colonies of *E. coli* survives even when sample is not diluted or
246 when 1:10 dilution is used. The higher amount of *E. coli* remaining in the test may indicate
247 that at higher pressures the degradation of the meropenem is more efficient and leads to
248 intermediates that are more oxidized than at lower pressurization and that due to its greater
249 similarity to meropenem still they have an antibiotic effect. Therefore, these results indicate
250 that the use of pressurized system does not only improve the degradation of antibiotics, but it
251 also helps to decrease the chemical risk of the treated urine by contributing to a more efficient
252 degradation of the raw pharmaceutical compound and its conversion into molecules with no
253 antibiotic effect.



254

255 **Figure 2.** Antibiotic activity (in terms of CFU ml⁻¹ of *E. coli*) and remaining meropenem
 256 concentration of synthetic urine after EF at different pressurizations. Electric charge passed:
 257 0.6 Ah dm⁻³. Experimental conditions: $j= 5.0 \text{ mA cm}^{-2}$, $\text{pH}_0= 3.0$, $[\text{meropenem}]_0 = 50.0 \text{ mg}$
 258 dm^{-3} , $[\text{goethite}] = 10.8 \text{ g}$.

259

260 As mentioned before, urine is a complex media in which organic and inorganic species
 261 coexist. These species are biodegradable and/or do not pose a risk to the environment and,
 262 thus, they are not considered as target compounds to be oxidized. Therefore, the effort should
 263 be focused on the search for efficient and selective processes towards antibiotics. To check
 264 this, Figure 3 shows the concentration profile (in terms of mg C L⁻¹) in semilogarithmic scale
 265 of meropenem and of the other organic naturally contained in urine: uric acid, creatinine, and
 266 urea. The total organic carbon is also shown in the figure, as indicator of the mineralization
 267 of the organic load.

268 As can be observed, meropenem degradation rate increases with the gauge pressure and after
 269 passing an electric charge of 0.8 Ah dm⁻³ the meropenem removals are 80.60%, 89.03%,

270 91.6% and 94.64% at gauge pressures of 0.0, 1.0, 2.0 and 3.0 bar, respectively. These decays
271 fit well to a first order kinetics Eq. (1) and kinetic constants are summarized in Table 1, where
272 it is noted the effect of the important effect of the gauge pressure applied (values higher than
273 70 % when pressure increases from atmospheric pressure to 3 bar of gauge pressure).

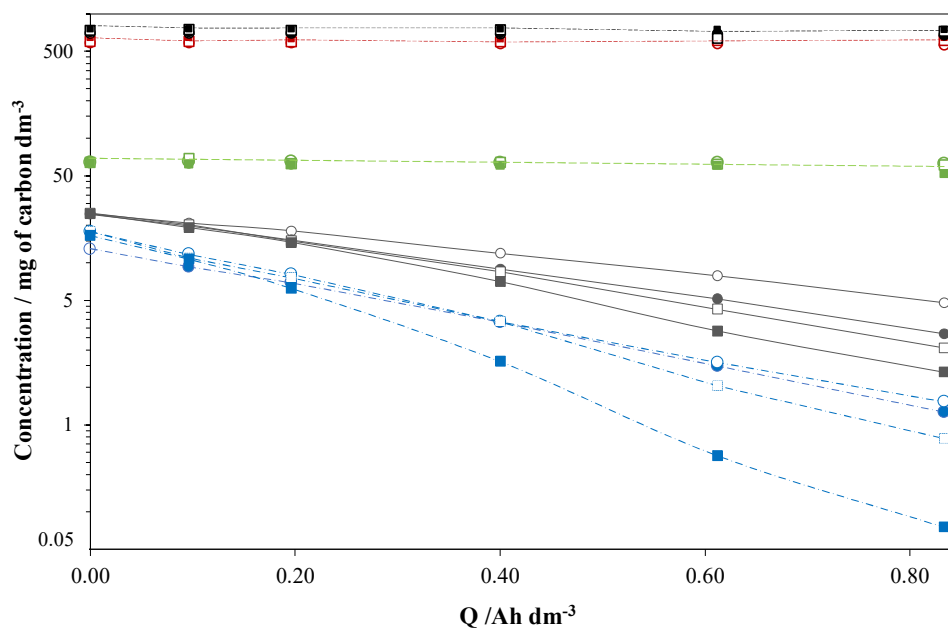
$$274 \quad \text{Ln}(C/C_0) = -k \cdot t \quad (1)$$

275 **Table 1.** Kinetic constants for meropenem decay by EF process at different overpressures.

Process	$k_{\text{MRP}} / \text{min}^{-1}$	R^2
EF 0.0 bar	0.0033	0.9965
EF 1.0 bar	0.0045	0.9982
EF 2.0 bar	0.0050	0.9964
EF 3.0 bar	0.0057	0.9916

276

277 Uric acid is also quickly oxidized. This was also observed in previous studies in which
278 electrochemical oxidation of synthetic urine was tested [28] and where it was pointed out that
279 this compound decomposes rapidly by light [29]. This can explain its faster depletion during
280 both electrochemical treatments. Regarding urea and creatinine, they are present in higher
281 concentration than uric acid and meropenem, and their concentrations almost remain constant
282 regardless of the gauge pressure applied. This agrees with the almost nil mineralization
283 observed, explained by the much higher concentration of these species in urine.



284

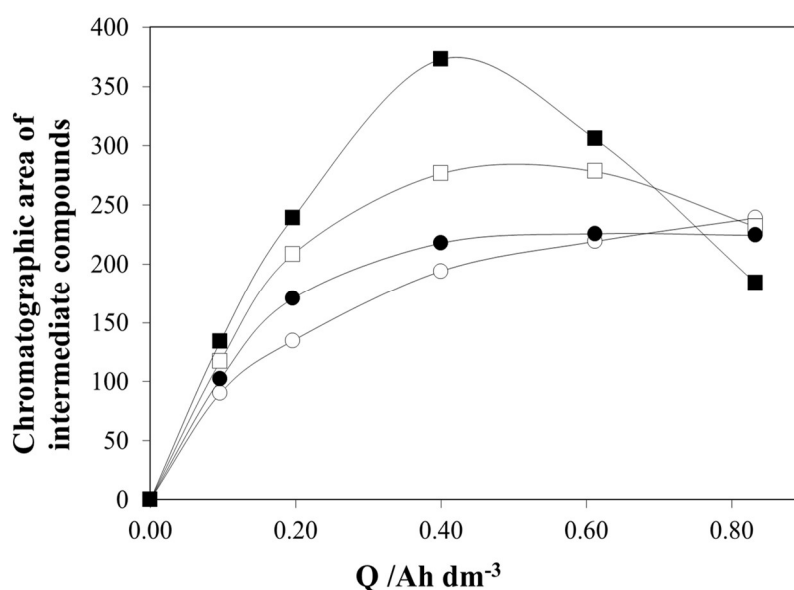
285 **Figure 3.** Influence of the overpressure on degradation of TOC, meropenem and organic
 286 compounds present in the synthetic urine in semilogarithmic scale as function of the applied
 287 electric charge during the EF tests. Experimental conditions: $j = 5.0 \text{ mA cm}^{-2}$, $\text{pH}_0 = 3.0$,
 288 $[\text{meropenem}]_0 = 50.0 \text{ mg dm}^{-3}$, $[\text{goethite}] = 10.8 \text{ g}$. Symbols: \circ 0.0 bar, \bullet 1.0 bar, \square 2.0 bar,
 289 \blacksquare 3.0 bar. Colours: \blacksquare Urea, \blacksquare TOC, \blacksquare Creatinine, \blacksquare Meropenem, \blacksquare Uric acid.

290

291 Figure 4 shows the trend of M1 ($\text{C}_{16}\text{H}_{27}\text{N}_3\text{O}_5\text{S}$), the main aromatic intermediate detected in
 292 the reaction system during EF process at the four pressures tested and identified by LC-MS
 293 (further data about this species are given below). Its concentration (expressed in terms of
 294 chromatographic area) increases with the gauge pressure applied and this agrees with the faster
 295 degradation of meropenem observed previously. Additionally, at a gauge pressure of 3 bar it
 296 attains a maximum value for 0.4 Ah dm^{-3} of electric charge passed and then it starts to decrease.
 297 That is, it behaves as reaction intermediate. In the EF at atmospheric pressure, this decrease
 298 is not observed. In this case, the degradation of meropenem is slower and around 20% of the
 299 initial meropenem still remains in the solutions after passing 0.8 Ah dm^{-3} of electric charge.
 300 Simultaneously, the formation of short-chain carboxylic acids is also observed, and their

301 trends are shown in Figure 5. As it is shown, a mixture of carboxylic acids is formed during
302 the treatment and their concentrations increase with the electrical charge passed. Among them,
303 propionic acid and acetic acid are the compounds accumulated in higher concentration in the
304 reaction system, and their concentrations depend significantly on the experimental conditions:
305 higher gauge pressures applied seem to favour their formation.

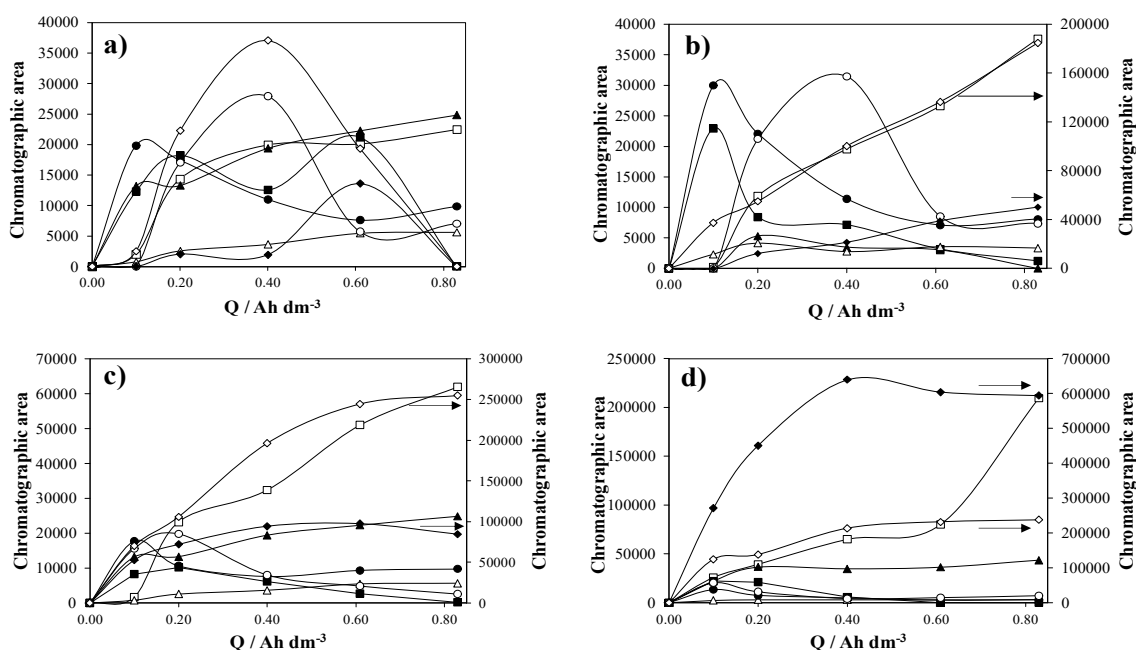
306



307

308 **Figure 4.** Chromatographic area of aromatic intermediate compounds as function of the
309 applied electric charge during the EF ~~Electro-Fenton~~ process at different overpressures. ○ 0
310 bar, ● 1.0 bar, □ 2.0 bar, ■ 3.0 bar. Experimental conditions: $j = 5.0 \text{ mA cm}^{-2}$, $\text{pH}_0 = 3.0$,
311 $[\text{meropenem}]_0 = 50.0 \text{ mg dm}^{-3}$, $[\text{goethite}] = 10.8 \text{ g}$.

312



313

314 **Figure 5.** Evolution of carboxylic acids concentration during EF process ~~Electro-Fenton test~~

315 at different overpressures. a) 0.0 bar, b) 1.0 bar, c) 2.0 bar and d) 3.0 bar. □ Oxalic Acid, ■

316 Maleic acid, ▲ Oxamic acid, Δ Malonic acid, ● Succinic acid, ○ Formic acid, ◆ Acetic acid,

317 ◇ Propionic acid. Experimental conditions: $j = 5.0 \text{ mA cm}^{-2}$, $\text{pH}_0 = 3.0$, $[\text{meropenem}]_0 = 50.0$

318 mg dm^{-3} , $[\text{goethite}] = 10.8 \text{ g}$.

319

320 In this point, it is important to remark that the great variety of inorganic and organic species

321 in urine (which are in higher concentration than meropenem) makes difficult the analysis and

322 identification of its degradation intermediates by HPLC, and the formation of some of them

323 can be masked. To clarify this point, additional tests were carried out in perchloric acid, using

324 the same initial antibiotic concentration and ionic conductivity of the reaction media (Figure

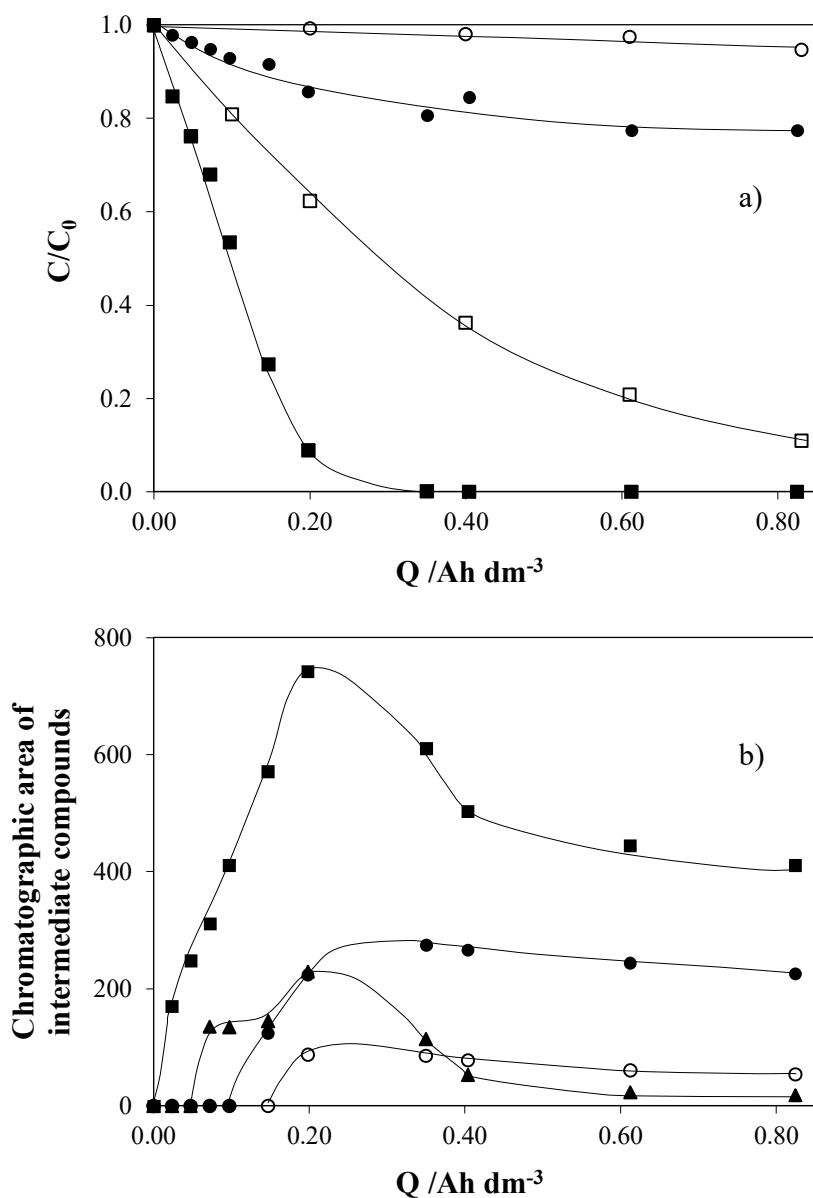
325 6). As can be observed, the degradation of meropenem is more efficient in perchloric acid and

326 0.4 Ah dm^{-3} of electric charge is enough to attain the complete removal of the antibiotic. This

327 confirms that in urine media there is a competitive oxidation and that electrons supplied are

328 not only use for the meropenem degradation, but for the oxidation of other compounds

329 contained in the solution including organics and inorganics. The oxidation of these ions can
330 lead to the formation of oxidants (such as hypochlorite, peroxosulfate or peroxodiphosphate)
331 that can contribute to the degradation (mediated oxidation) or recombine with each other [30]
332 without contributing to mediated oxidation. The complete mineralization of meropenem is
333 also promoted and up to 20 % of TOC removal is attained in perchloric media after 8.0 h of
334 treatment. This indicates that meropenem is rapidly oxidized but further reaction time is
335 required to attain the complete conversion of the organic load to carbon dioxide. That is, the
336 accumulation of reaction intermediates should take place. Part b of Figure 6 shows the main
337 aromatic intermediates detected and accumulated in the system during the degradation of
338 meropenem by EF process in perchloric acid media at a gauge pressure of 1 bar. Four aromatic
339 intermediates were identified by LC-MS (Table 2). As in the case of EF of urine, M1
340 ($C_{16}H_{27}N_3O_5S$) is the main intermediate which can be generated by hydrolysis of the aromatic
341 nitrile group. Comparing chromatographic area, the maximum concentration attained in
342 perchloric acid (data shown in Figure 6b) is higher than those monitored in urine media (data
343 shown in Figure 4), indicating that hydrolysis should be faster in perchloric acid, and this can
344 explain the rapid decay observed in meropenem concentration. Additionally, M2
345 ($C_{16}H_{25}N_3O_4S$), M3 ($C_{17}H_{27}N_3O_6S$), M4 ($C_{10}H_{19}NO_4$) and M5 ($C_{15}H_{27}N_3O_4S$) were also
346 identified. Wang et al. [31] also identified the intermediates M1 ($C_{16}H_{27}N_3O_5S$), M2
347 ($C_{16}H_{25}N_3O_4S$), M4 ($C_{10}H_{19}NO_4$) and M5 ($C_{15}H_{27}N_3O_4S$) during the photocatalytic removal
348 of meropenem. In the case of urine medium, M1 ($C_{16}H_{27}N_3O_5S$) was the only intermediate
349 detected by HPLC, but M2 ($C_{16}H_{25}N_3O_4S$) and M3 ($C_{16}H_{25}N_3O_4S$) were also detected by LC-
350 MS. In any case, analyzing these results together with those shown in Figure 2, these
351 intermediates do not seem to present antibiotic effect and then their discharge to the sewerage
352 system may not lead to serious environmental problems neither promote the appearance of
353 bacteria resistant to antibiotic.



354

355 **Figure 6.** a) Meropenem (■, □) and TOC removal (●, ○) as function of the applied electric
 356 charge during the EF of meropenem in urine (empty symbols) and perchloric acid (full
 357 symbols) media pressurized at 1.0 bar of gauge pressure. b) Chromatographic area of the
 358 aromatic intermediates formed during the EF of meropenem in perchloric acid media at 1 bar
 359 of overpressure. ■ M1 ($C_{16}H_{27}N_3O_5S$), ▲ M2 ($C_{16}H_{25}N_3O_4S$), ○ M3 ($C_{17}H_{27}N_3O_6S$), ● M4
 360 ($C_{10}H_{19}NO_4$). Experimental conditions: $j = 5.0 \text{ mA cm}^{-2}$, $\text{pH}_0 = 3.0$, $[\text{meropenem}]_0 = 50.0 \text{ mg}$
 361 dm^{-3} , $[\text{goethite}] = 10.8 \text{ g}$.

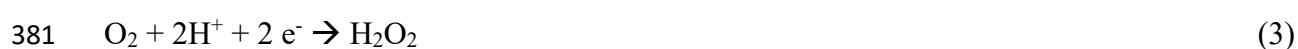
362

363 **Table 2.** Analytes identified, structure and m/z.

	Formula	m/z	Feasible structure
Meropenem	$C_{17}H_{25}N_3O_5S$	383.15149	
M1	$C_{16}H_{27}N_3O_5S$	373.16714	
M2	$C_{16}H_{25}N_3O_4S$	355.15658	
M3	$C_{17}H_{27}N_3O_6S$	401.16206	
M4	$C_{10}H_{19}NO_4$	217.13141	
M5	$C_{15}H_{27}N_3O_4S$	345.17223	

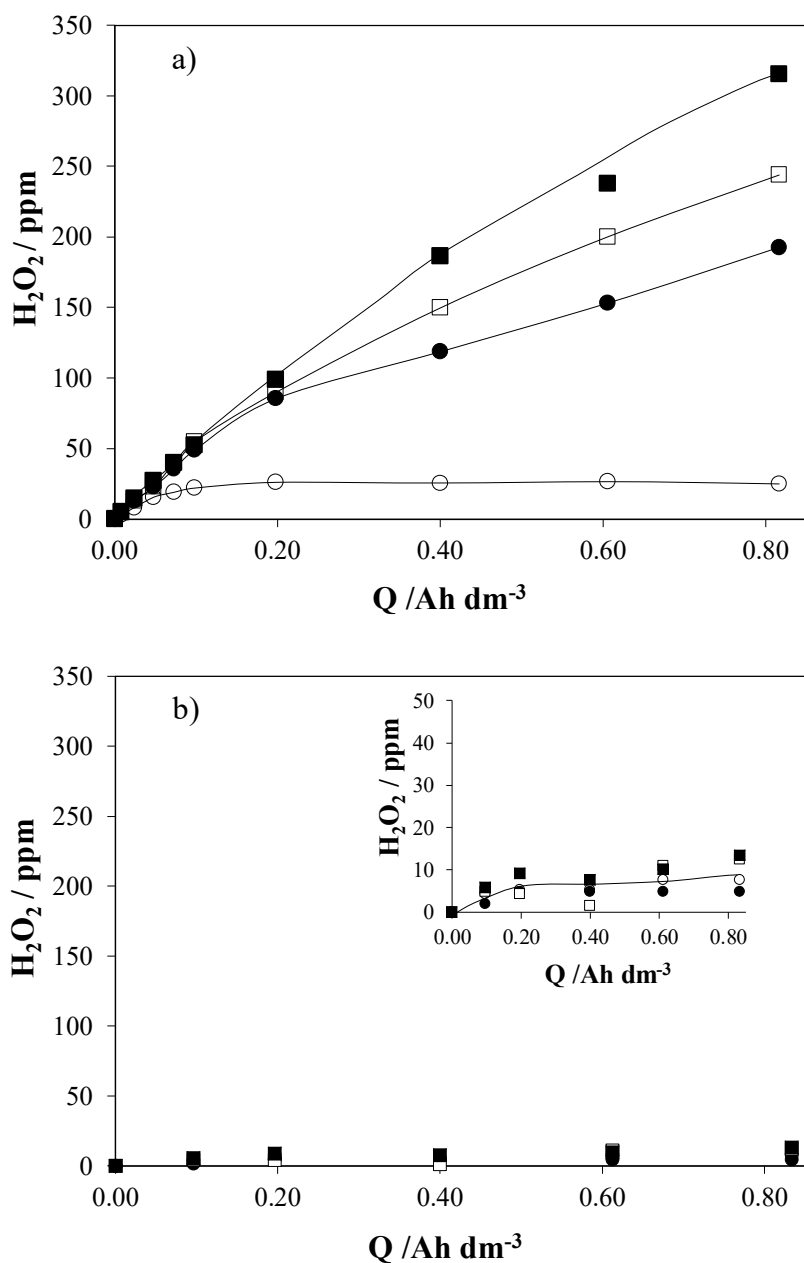
364

365 The positive effect of gauge pressure on meropenem degradation by EF may be related to the
366 contribution of direct and mediated oxidation mechanisms promoted in the electrochemical
367 system. As it is known, the generation of hydroxyl radicals via Fenton's reaction, Eq. (2)
368 depends on the concentration of hydrogen peroxide [19]. H₂O₂ is generated mainly by
369 reduction of O₂ on the cathode according to Eq. (3). Its generation rate depends on the current
370 intensity and electrode material, and it is often limited by the solubility of oxygen in water
371 [11]). Then, the addition of oxygen is key for a fast and efficient electro-generation of
372 hydrogen peroxide. As explained before, the experimental set up used in this work is equipped
373 with a jet aerator which was tested in previous works for the electro-generation of H₂O₂ [16,
374 32]. Results confirmed that the aerator based on venturi effect helps to super-saturate the
375 solution with oxygen even at atmospheric pressure. Additionally, it is important to take in
376 mind that the solubility of oxygen in water increases with pressure (linearly in the range
377 studied) according to Henry's Law. Then, the amount of dissolved oxygen in the liquid treated
378 is expected to be much higher at 3 bar, and therefore the electro-generation of hydrogen
379 peroxide should be promoted.



382

383 To confirm this, additional tests were carried out in urine media, without organic load and in
384 absence of catalyst, to prevent the fast decomposition of the electrogenerated hydrogen
385 peroxide. Figure 7a shows the changes in the concentration of hydrogen peroxide with the
386 applied electric charge at different gauge pressures applied (0.0, 1.0, 2.0 and 3.0 bar) when
387 applying a current density of 5.0 mA cm⁻². Additionally, Figure 7b shows the remaining
388 concentration of hydrogen peroxide during the EF tests of meropenem in urine media at
389 different gauge pressures applied.



390

391 **Figure 7.** a) Concentration of hydrogen peroxide generated as function of the applied electric
 392 charge at different overpressures in the absence of iron catalyst and organic compounds
 393 present in the urine. b) Concentration of hydrogen peroxide remain in the system during the
 394 EF of meropenem in urine media. Experimental conditions: $j= 5.0 \text{ mA cm}^{-2}$, $\text{pH}_0= 3.0$,
 395 $[\text{meropenem}]_0$ in EF tests = 50.0 mg dm^{-3} , $[\text{goethite}]$ in EF tests = 10.8 g . \circ 0.0 bar, \bullet 1.0 bar,
 396 \square 2.0 bar, \blacksquare 3.0 bar

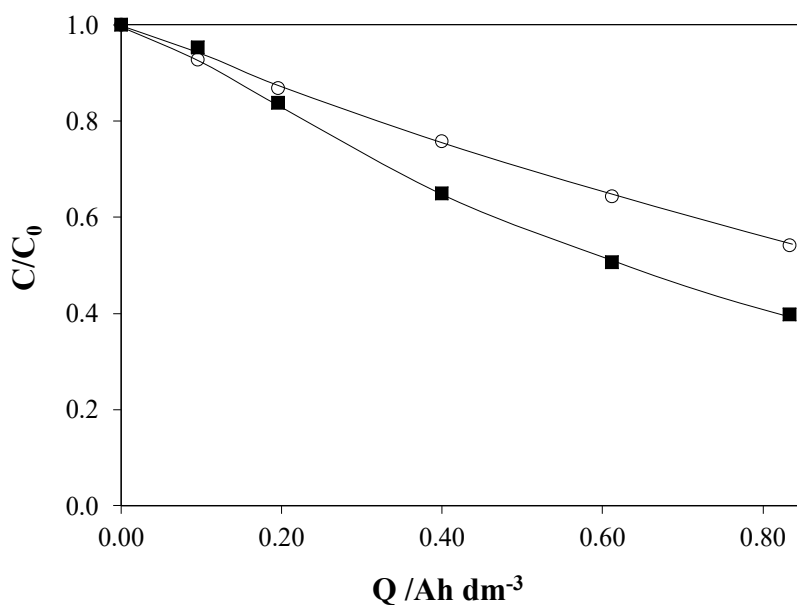
397 As can be observed, hydrogen peroxide concentration increases with the applied electric
398 charge and gauge pressure. The maximum amounts obtained are 24.99, 192.61, 244.01 and
399 315.37 mg dm⁻³, for 0.0, 1.0, 2.0 and 3.0 bar, respectively. Two regions are observed in the
400 generation of hydrogen peroxide regardless of the gauge pressure applied. Initially, hydrogen
401 peroxide increases rapidly but its concentration starts to stabilize from a given electric charge
402 passed. This indicates that other parasitic reactions occur such as its self-decomposition (Eq.
403 4), or its oxidation to oxygen in the anode (Eq. 5) or reduction to water in the cathode (Eq. 6)
404 [11, 18, 33]. Initially, the rate of these side reactions is low because of the low hydrogen
405 peroxide concentration but after that, they start to be relevant, and the generation rate is no
406 longer linear. Then, the plateau zone attained indicates that formation and decomposition
407 reaction rates balance.



411 At atmospheric pressure, the accumulation reaches the plateau after passing 0.1 Ah dm⁻³.
412 However, for gauge pressures applied of 1.0, 2.0 and 3.0 bar, the oxygen concentration is high
413 enough to guaranty a higher generation rate in comparison with decomposition ones and 0.8
414 Ah dm⁻³ are not enough to attain this plateau. In comparing these results with the concentration
415 of hydrogen peroxide during EF processes (part b of Figure 7), it can be observed that in all
416 cases the residual concentration is low (around 10-15 ppm) and negligible differences are
417 observed with the gauge pressure applied. Then, regardless of the H₂O₂ generated, this oxidant
418 seems to be rapidly activated and this can help to explain the better results obtained in
419 pressurized-EF where the amount of hydrogen peroxide generated and activated should be
420 higher. Additionally, it is important to mention that leaching does not seem to be favored with
421 gauge pressure and in any case soluble iron species are detected in the media.

422 Besides cathodic generation of hydrogen peroxide, the anodic reaction can also contribute to
423 the overall degradation process and the effect of gauge pressure applied on it should be also
424 checked. Figure 8 shows the degradation of meropenem in urine media during
425 electrooxidation in the same cell, but without aeration, at atmospheric pressure and with 1.0
426 bar of gauge pressure. As it can be observed, electrochemical oxidation is also improved
427 working at 1 bar and around 14 % extra of meropenem is oxidized during the test. Oxygen
428 produced during the anodic oxidation of water (typically the non-desired side reaction) can be
429 more efficiently dissolved into the liquid in treatment and, hence, a higher amount of oxygen
430 is available on the cathode for the generation of hydrogen peroxide.

431



432

433 **Figure 8.** Meropenem removal as function of the applied electric charge during the
434 electrooxidation of synthetic urine. Experimental conditions: $j= 5.0 \text{ mA cm}^{-2}$, $\text{pH}_0= 3.0$,
435 $[\text{meropenem}]_0= 50.0 \text{ mg dm}^{-3}$. (○) atmospheric pressure, (■) pressurized with 1.0 bar of gauge
436 pressure.

437

438 Hence, from the obtained results it can be concluded that the use of pressurized EF reactors
439 can allow to increase the efficiency of EF processes, and that it can be satisfactorily used to
440 degrade selectivity antibiotics in urine media. Pressurized EF has been previously tested in
441 the recent years [9, 18, 21, 34] but these works employed very different electrochemical
442 reactors (mixed tanks cells) and they were focused on the improvement of the mineralization
443 of the process using up to 10 and 30 bar of gauge pressure. Table 3 summarizes the
444 experimental conditions and the main results reported previously in literature. The direct
445 comparison of these results is not an easy task due to the different experimental conditions
446 tested, aqueous matrix, electrodic material used, catalyst used, or electrical charge passed. In
447 any case, as for the knowledge of the authors, this is the first time in which the use of
448 moderated pressurized EF has been satisfactorily tested to decrease the chemical risk of
449 hospital effluents.

450

451

452

453

454

455

456

457

458

459

460

461

Table 3. Experimental conditions and the main results reported previously in literature

Process	Conditions	Target	Initial concentration	Results	Kinetic constant	Ref.
Homogeneous EF	Microfluidic Flow-Through reactor at atmospheric pressure. <i>Anode:</i> 3D-Boron Doped Diamond (BDD) mesh <i>Cathode:</i> modified 3D-Aluminium foam (Al) with CB/PTFE or modified 3D-RVC foam with CB/PTFE. <i>Current density:</i> 10 mA cm ⁻² <i>Electrolyte:</i> 7 mM Na ₂ SO ₄ at pH 3, Fe ²⁺ (0.5 mM).	Clopyralid	100.0 mg dm ⁻³	3D-Al-CB/PTFE: 100% removal (0.44 Ah dm ⁻³) 3D-RVC-CB/PTFE: 100% removal (0.90 Ah dm ⁻³)	-	[35]
EO or Homogeneous EF	Two types of electrochemical cells: Commercial flow-by and Microfluidic Flow-Through reactor. Atmospheric pressure. <i>Anode:</i> 3D-BDD mesh <i>Cathode:</i> Stainless Steel (EO) or modified 3D-Aluminium foam with CB/PTFE (EF). <i>Current density:</i> 10 mA cm ⁻² <i>Electrolyte:</i> soil washing fluids at pH 3, <i>Catalyst in EF tests:</i> Fe ²⁺ (0.5 mM)	Clopyralid	400 g of soil polluted with 100 g kg ⁻¹ with 1.0 dm ³ of water	<u>Commercial flow-by:</u> Electrooxidation: 80% removal (6.0 Ah dm ⁻³) <u>Microfluidic Flow-Through reactor:</u> Electrooxidation: 80% removal (4.0 Ah dm ⁻³) Electro-Fenton: 80% removal (0.4 Ah dm ⁻³)	-	[36]
Heterogeneous EF	Microfluidic Flow-Through reactor at atmospheric pressure. <i>Anode:</i> BDD mesh <i>Cathode:</i> modified titanium mesh with CB/PTFE. 6 g of iron (Fe ³⁺) containing alginate beads <i>Current:</i> 0.12 and 0.25 A <i>Electrolyte:</i> 0.05 M Na ₂ SO ₄ at pH 3.	Clofibrilic acid	10.0 mg dm ⁻³	0.12 A~100% removal (8h) 0.25 A~100% removal (8h)	0.009 min ⁻¹ (0.12 A) 0.014 min ⁻¹ (0.25 A)	[32]

Homogeneous EF	Undivided high-pressure stainless-steel cell Pressurised system. <i>Anode: Ti/IrO₂-Ta₂O₅</i> <i>Cathode: compact graphite</i> <i>Electrolyte: 35 mM Na₂SO₄ at pH 3</i> <i>Catalyst: 0.5 mM Fe(SO)₄ at pH 3</i> <i>Current: 110 mA</i> <i>Range of gauge pressures: 0, 3, 6 and 11 bar</i>	Acid Orange 7	0.43 mM	0 bar: 48 % removal of TOC 3 bar: 54 % removal of TOC 6 bar: 63 % removal of TOC 10 bar: 74 % removal of TOC	-	[18]
Homogeneous EF	Undivided high-pressure stainless-steel cell Pressurised system <i>Anode: DSA[®]</i> <i>Cathode: carbon felt</i> <i>Current density: 20 mA cm⁻²</i> <i>Electrolyte: real paper mill wastewater at pH 3</i> <i>Catalyst: Fe²⁺ 0.5 mM</i> <i>Range of gauge pressures: 0 and 10 bar</i>	Real wastewater	115.0 mg dm ⁻³ TOC	0 bar: 48 % removal of TOC (5h) 10 bar: 58 % removal of TOC (5h)	-	[21]
Homogeneous EF	Undivided high-pressure stainless-steel cell Pressurised system <i>Anode: Ti/IrO₂-Ta₂O₅</i> <i>Cathode: carbon felt</i> <i>Current density: 10 mA cm⁻²</i> <i>Electrolyte: 50 mM Na₂SO₄ at pH 3</i> <i>Catalyst: Fe²⁺ 0.5 mM</i> <i>Range of gauge pressures: 0 and 30 bar</i>	Maleic Acid	0.70 mM	0 bar: 40 % removal (2h) 30 bar: 90 % removal (4h)	-	[9]
Homogeneous or heterogeneous EF	Undivided high-pressure stainless-steel cell Pressurised system with oxygen <i>Anode: Ti/IrO₂-Ta₂O₅</i> <i>Cathode: carbon felt</i> <i>Current density: 20 mA cm⁻²</i> <i>Electrolyte: 0.1 M Na₂SO₄ at pH 3</i> <i>Catalyst: Fe²⁺ (0.05 M), pyrite (1.0 g L⁻¹) and chalcopyrite (0.5 g L⁻¹)</i> <i>Range of gauge pressures: 1 and 10 bar</i>	Caffeic Acid	100.0 mg dm ⁻³	<u>Fe²⁺</u> : 1 bar: 30% removal of TOC (2h) 10 bar: 58% removal of TOC (2h) <u>Pyrite</u> : 1 bar: ~40% removal of TOC (2h) 10 bar: ~58% removal of TOC (2h) <u>Chalcopyrite</u> : 1 bar: ~48% removal of TOC (2h) 10 bar: ~74% removal of TOC (2h)	-	[19]

Heterogeneous EF	<p>Microfluidic Flow-Through reactor. Pressurised system. <i>Anode:</i> 3D-MMO-IrO₂Ta₂O₅ mesh <i>Cathode:</i> Modified 3D-titanium mesh with CB/PTFE. 10.8 g of goethite. <i>Current density:</i> 5 mA cm⁻² <i>Electrolyte:</i> Urine at pH 3 <i>Range of gauge pressures:</i> 0 to 3 bar</p>	Meropenem	50.0 mg dm ⁻³	<p>0 bar: 80.60 % removal 1 bar: 89.03 % removal 2 bar: 91.60 % removal 3 bar: 94.64 % removal</p>	<p>0.0033 min⁻¹ (0 bar) 0.0045 min⁻¹ (1 bar) 0.0050 min⁻¹ (2 bar) 0.0057 min⁻¹ (3 bar)</p>	This work
------------------	--	-----------	--------------------------	---	---	-----------

463

464

465

466

467

468

469

470

471

472

473

474 4. CONCLUSIONS

475 From this work, the following conclusions can be drawn:

- 476 • Meropenem can be degraded by EF in system in which jet aerator, microfluid flow
477 through cell and iron bed are implemented. The abatement of meropenem is related
478 to the antibiotic effect (quantified using *E. coli* as target bacterium) remained in the
479 treated urine but it cannot fully explain the decay in the antibiotic capacity of the
480 treated urine.
- 481 • The mineralization is almost nil during EF of polluted urine at 5.0 mA cm⁻² using
482 goethite as heterogeneous catalyst. Increasing pressurization is not relevant in terms
483 of TOC removal but it favours the progress of the degradation as it is demonstrated
484 with the accumulation of carboxylic acids in the treated urine. In addition, it has a
485 positive effect on the losing of antibiotic capacity of the treated urine, which is
486 explained in terms of the higher progress of the oxidation reached.
- 487 • The positive effect of the pressurization on EF is related to the higher hydrogen
488 peroxide generation in pressurized systems, which in turn is explained in terms of the
489 higher oxygen concentration that can be attained. Additionally, the anodic oxidation
490 is also favoured because the formation of oxygen from the non-desired water oxidation
491 provides of oxygen to the cathode for the effective production of hydrogen peroxide.

492

493 ACKNOWLEDGEMENTS

494 Financial support from Junta de Comunidades de Castilla-La Mancha (JCCM), European
495 Union (European Regional Development Fund), and Ministry of Science and Innovation
496 through the projects SBPLY/17/180501/000396 and PID2019-110904RB-I00 are gratefully
497 acknowledged. The Spanish Ministry of Economy, Industry, and Competitiveness and the
498 European Union is also gratefully acknowledged through the projects EQC2018-004469-P
499 and EQC2018-004240-P.

500 REFERENCES

- 501 [1] H. Wang, H. Xi, L. Xu, M. Jin, W. Zhao, H. Liu, Ecotoxicological effects, environmental fate and
502 risks of pharmaceutical and personal care products in the water environment: A review, *Science of*
503 *The Total Environment*, 788 (2021) 147819.
- 504 [2] U. Szymańska, M. Wiergowski, I. Sołtyszewski, J. Kuzemko, G. Wiergowska, M.K. Woźniak,
505 Presence of antibiotics in the aquatic environment in Europe and their analytical monitoring: Recent
506 trends and perspectives, *Microchemical Journal*, 147 (2019) 729-740.
- 507 [3] I. Sirés, E. Brillas, M.A. Oturan, M.A. Rodrigo, M. Panizza, Electrochemical advanced oxidation
508 processes: today and tomorrow. A review, *Environmental Science and Pollution Research*, 21 (2014)
509 8336-8367.
- 510 [4] W. Wang, Y. Li, Y. Li, M. Zhou, O.A. Arotiba, Electro-Fenton and photoelectro-Fenton
511 degradation of sulfamethazine using an active gas diffusion electrode without aeration, *Chemosphere*,
512 250 (2020) 126177.
- 513 [5] H. Pourzamani, N. Mengelizadeh, H. Mohammadi, N. Niknam, B. Neamati, R. Rahimi,
514 Comparison of electrochemical advanced oxidation processes for removal of ciprofloxacin from
515 aqueous solutions, *Desalination and Water Treatment*, 113 (2018) 307-318.
- 516 [6] E. Brillas, I. Sirés, M.A. Oturan, Electro-Fenton Process and Related Electrochemical
517 Technologies Based on Fenton's Reaction Chemistry, *Chemical Reviews*, 109 (2009) 6570-6631.
- 518 [7] P.V. Nidheesh, R. Gandhimathi, Trends in electro-Fenton process for water and wastewater
519 treatment: An overview, *Desalination*, 299 (2012) 1-15.
- 520 [8] I. Sirés, E. Brillas, Upgrading and expanding the electro-Fenton and related processes, *Current*
521 *Opinion in Electrochemistry*, 27 (2021) 100686.
- 522 [9] J.F. Pérez, S. Sabatino, A. Galia, M.A. Rodrigo, J. Llanos, C. Sáez, O. Scialdone, Effect of air
523 pressure on the electro-Fenton process at carbon felt electrodes, *Electrochimica Acta*, 273 (2018) 447-
524 453.
- 525 [10] F. Yu, M. Zhou, X. Yu, Cost-effective electro-Fenton using modified graphite felt that
526 dramatically enhanced on H₂O₂ electro-generation without external aeration, *Electrochimica Acta*, 163
527 (2015) 182-189.
- 528 [11] J.F. Pérez, J. Llanos, C. Sáez, C. López, P. Cañizares, M.A. Rodrigo, Towards the scale up of a
529 pressurized-jet microfluidic flow-through reactor for cost-effective electro-generation of H₂O₂, *Journal*
530 *of Cleaner Production*, 211 (2019) 1259-1267.
- 531 [12] G.d.O.S. Santos, K.I.B. Eguiluz, G.R. Salazar-Banda, C. Saez, M.A. Rodrigo, Testing the role of
532 electrode materials on the electro-Fenton and photoelectro-Fenton degradation of clopyralid, *Journal*
533 *of Electroanalytical Chemistry*, 871 (2020) 114291.
- 534 [13] R.R. Kalantary, M. Farzadkia, M. Kermani, M. Rahmatinia, Heterogeneous electro-Fenton
535 process by Nano-Fe₃O₄ for catalytic degradation of amoxicillin: Process optimization using response
536 surface methodology, *Journal of Environmental Chemical Engineering*, 6 (2018) 4644-4652.
- 537 [14] Y. Jiao, L. Ma, Y. Tian, M. Zhou, A flow-through electro-Fenton process using modified activated
538 carbon fiber cathode for orange II removal, *Chemosphere*, 252 (2020) 126483.
- 539 [15] V.S. Pinheiro, E.C. Paz, L.R. Aveiro, L.S. Parreira, F.M. Souza, P.H.C. Camargo, M.C. Santos,
540 Mineralization of paracetamol using a gas diffusion electrode modified with ceria high aspect ratio
541 nanostructures, *Electrochimica Acta*, 295 (2019) 39-49.
- 542 [16] J.F. Pérez, J. Llanos, C. Sáez, C. López, P. Cañizares, M.A. Rodrigo, The jet aerator as oxygen
543 supplier for the electrochemical generation of H₂O₂, *Electrochimica Acta*, 246 (2017) 466-474.
- 544 [17] F. Yu, Y. Chen, Y. Pan, Y. Yang, H. Ma, A cost-effective production of hydrogen peroxide via
545 improved mass transfer of oxygen for electro-Fenton process using the vertical flow reactor,
546 *Separation and Purification Technology*, 241 (2020) 116695.
- 547 [18] O. Scialdone, A. Galia, C. Gattuso, S. Sabatino, B. Schiavo, Effect of air pressure on the electro-
548 generation of H₂O₂ and the abatement of organic pollutants in water by electro-Fenton process,
549 *Electrochimica Acta*, 182 (2015) 775-780.
- 550 [19] A.H. Ltaïef, S. Sabatino, F. Proietto, S. Ammar, A. Gadri, A. Galia, O. Scialdone, Electrochemical
551 treatment of aqueous solutions of organic pollutants by electro-Fenton with natural heterogeneous
552 catalysts under pressure using Ti/IrO₂-Ta₂O₅ or BDD anodes, *Chemosphere*, 202 (2018) 111-118.

553 [20] J.F. Pérez, A. Galia, M.A. Rodrigo, J. Llanos, S. Sabatino, C. Sáez, B. Schiavo, O. Scialdone,
554 Effect of pressure on the electrochemical generation of hydrogen peroxide in undivided cells on carbon
555 felt electrodes, *Electrochimica Acta*, 248 (2017) 169-177.

556 [21] N. Klidi, F. Proietto, F. Vicari, A. Galia, S. Ammar, A. Gadri, O. Scialdone, Electrochemical
557 treatment of paper mill wastewater by electro-Fenton process, *Journal of Electroanalytical Chemistry*,
558 841 (2019) 166-171.

559 [22] E.A. Agudelo, S.A. Cardona G, Advanced Oxidation Technology (Ozone-catalyzed by Powder
560 Activated Carbon - Portland Cement) for the Degradation of the Meropenem Antibiotic, *Ozone:*
561 *Science & Engineering*, 43 (2021) 88-105.

562 [23] J.F. Pérez, J. Llanos, C. Sáez, C. López, P. Cañizares, M.A. Rodrigo, Development of an
563 innovative approach for low-impact wastewater treatment: A microfluidic flow-through
564 electrochemical reactor, *Chemical Engineering Journal*, 351 (2018) 766-772.

565 [24] S. Dbira, N. Bensalah, P. Cañizares, M.A. Rodrigo, A. Bedoui, The electrolytic treatment of
566 synthetic urine using DSA electrodes, *Journal of Electroanalytical Chemistry*, 744 (2015) 62-68.

567 [25] S. Cotillas, E. Lacasa, C. Sáez, P. Cañizares, M.A. Rodrigo, Disinfection of urine by conductive-
568 diamond electrochemical oxidation, *Applied Catalysis B: Environmental*, 229 (2018) 63-70.

569 [26] G. Eisenberg, Colorimetric Determination of Hydrogen Peroxide, *Industrial & Engineering*
570 *Chemistry Analytical Edition*, 15 (1943) 327-328.

571 [27] E.C.o.A.S. Testing, "The European Committee on Antimicrobial Susceptibility Testing.
572 Breakpoint tables for interpretation of MICs and zone diameters. Version 11.0, 2021.

573 [28] M. Herraiz-Carboné, S. Cotillas, E. Lacasa, Á. Moratalla, P. Cañizares, M.A. Rodrigo, C. Sáez,
574 Improving the biodegradability of hospital urines polluted with chloramphenicol by the application of
575 electrochemical oxidation, *Science of The Total Environment*, 725 (2020) 138430.

576 [29] M. Herraiz-Carboné, S. Cotillas, E. Lacasa, P. Cañizares, M.A. Rodrigo, C. Sáez, Enhancement
577 of UV disinfection of urine matrixes by electrochemical oxidation, *Journal of Hazardous Materials*,
578 (2020) 124548.

579 [30] I.M.D. Gonzaga, A. Moratalla, K.I.B. Eguiluz, G.R. Salazar-Banda, P. Cañizares, M.A. Rodrigo,
580 C. Saez, Influence of the doping level of boron-doped diamond anodes on the removal of penicillin G
581 from urine matrixes, *Science of The Total Environment*, 736 (2020) 139536.

582 [31] J. Wang, B. Gao, M. Dou, X. Huang, Z. Ma, A porous g-C₃N₄ nanosheets containing nitrogen
583 defects for enhanced photocatalytic removal meropenem: Mechanism, degradation pathway and DFT
584 calculation, *Environmental Research*, 184 (2020) 109339.

585 [32] V. Poza-Nogueiras, Á. Moratalla, M. Pazos, Á. Sanromán, C. Sáez, M.A. Rodrigo, Towards a
586 more realistic heterogeneous electro-Fenton, *Journal of Electroanalytical Chemistry*, 895 (2021)
587 115475.

588 [33] E. Petrucci, A. Da Pozzo, L. Di Palma, On the ability to electrogenerate hydrogen peroxide and
589 to regenerate ferrous ions of three selected carbon-based cathodes for electro-Fenton processes,
590 *Chemical Engineering Journal*, 283 (2016) 750-758.

591 [34] N. Hamdi, F. Proietto, H. Ben Amor, A. Galia, R. Inguanta, S. Ammar, A. Gadri, O. Scialdone,
592 Effective Removal and Mineralization of 8-Hydroxyquinoline-5-sulfonic Acid through a Pressurized
593 Electro-Fenton-like Process with Ni-Cu-Al Layered Double Hydroxide, *ChemElectroChem*, 7 (2020)
594 2457-2465.

595 [35] J.F. Pérez, J. Llanos, C. Sáez, C. López, P. Cañizares, M.A. Rodrigo, On the design of a jet-
596 aerated microfluidic flow-through reactor for wastewater treatment by electro-Fenton, *Separation and*
597 *Purification Technology*, 208 (2019) 123-129.

598 [36] M. Rodríguez, M. Muñoz-Morales, J.F. Perez, C. Saez, P. Cañizares, C.E. Barrera-Díaz, M.A.
599 Rodrigo, Toward the Development of Efficient Electro-Fenton Reactors for Soil Washing Wastes
600 through Microfluidic Cells, *Industrial & Engineering Chemistry Research*, 57 (2018) 10709-10717.

601